



Contents lists available at ScienceDirect

Journal of Photochemistry and Photobiology A: Chemistry

journal homepage: www.elsevier.com/locate/jphotochem

The effects of central metals and peripheral substituents on the photophysical properties and optical limiting performance of phthalocyanines with axial chloride ligand

Jun Chen, Quan Gan, Shayu Li, Fangbin Gong, Qian Wang, Zhipei Yang, Shuangqing Wang*, Huijun Xu, Jin Shi Ma, Guoqiang Yang*

Beijing National Laboratory for Molecular Sciences, CAS Key Laboratory of Photochemistry, Institute of Chemistry, The Chinese Academy of Sciences, Beijing 100190, PR China

ARTICLE INFO

Article history:

Available online 3 May 2009

Keywords:

Metal phthalocyanine
Photophysics
Optical limiting
Axial substituent

ABSTRACT

A series of peripherally substituted phthalocyanines (Pcs) with different central metals (Al, Ga and In) and axial chloride ligand were synthesized and their photophysical and optical limiting properties were investigated. The Q band absorption of the Pc shifts to longer wavelength with the central metals changing from Al to In, and the fluorescence quantum yields of S_1 emission decrease remarkably from Al to In. Transient absorption spectra of the Pcs in THF were measured in determination of the photophysical parameters. The optical limiting properties were investigated by a nanosecond pulse laser at 532 nm. All of these compounds exhibit good optical limiting performance, and the optical limiting behaviors of solid solution in glass obtained by sol-gel technique are much better than that of liquid solution. Several factors which affect the optical limiting performance of the Pcs with different central metals and substituents are discussed.

© 2009 Published by Elsevier B.V.

1. Introduction

Nonlinear optical materials are continuously attracting attention for their potential applications in many fields such as optical storage, optical communications and optical limiting, etc. [1–3]. Among the large number of optical limiters, phthalocyanines (Pcs) are found to be outstanding optical limiting materials because of their special structures of two-dimensional highly conjugated delocalized π -electron system and metal-conjugant bond [4–7].

The optical limiting material can effectively attenuate glaring laser and dangerous optical beam, allowing only a reduced transmission to the target area. Therefore it may protect human eyes and optical sensors from being damaged [8–11]. For all favorable optical limiting materials, strong nonlinear absorption, nonlinear refraction or nonlinear dispersion are exhibited to reduce the input laser to suitable output intensity [12,13]. Pcs are typical compounds with suitable photophysical properties which result in excellent reverse saturable absorption for optical limiting and nonlinear transmittance application [14–17]. The occurrence of the reverse saturable absorption requires that the excited absorption cross section σ_{ex} is greater than that of the ground state σ_g [18–20]. For the practical applications of optical limiting and nonlinear transmittance effect, it is desirable to have reverse saturable absorbers, which

allow high transmission of light at low optical fields over a large spectral window [21,22]. For the Pcs, the optical window of transient absorption occurs from 400 to 600 nm between the Q and B bands of the Pcs' ground state absorption. Introduction of central metals and peripherally substituted groups will effectively enlarge the optical window for optical limiting and nonlinear transmittance behaviors [23,24]. Among all investigation of the optical limiting materials, the essential condition of achieving preferable optical limiting properties is that the compounds in system could not be aggregated or only have little aggregation [25,26]. However, most of the Pcs are easy to be aggregated and have poor solubility in common solvents because of strong interactions between the Pc molecules. So reducing the aggregation and improving the solubility of the Pcs are important research works to achieve favorable optical limiting materials. Introduction of substituted groups is one of effective ways of improving the solubility of the Pcs, and also different substituents may cause different effects on the photophysical and optical limiting properties of the Pcs [27,28]. The axially substituted halogen atom which connect to the central metal could greatly influence the solubility and optical limiting behaviors of the Pcs [29,30]. Moreover, the central metals also play important roles in the properties of Pcs, and change the optical limiting behaviors [29,31]. The photophysical properties of Pcs can be modulated by altering the peripheral and axial substituents, central metals as well as the structures of the macrocyclic rings [32,33].

So far many researches have been focused on the effects of substituents or the central metals on the photophysical and optical

* Corresponding authors. Fax: +86 10 82617315.

E-mail addresses: g1704@iccas.ac.cn (S. Wang), gqyang@iccas.ac.cn (G. Yang).

limiting properties of the Pcs [5,34,35], and provided some useful guidelines. However, up to now, Pc-based materials are still being investigated to improve their optical limiting performance for the practical application. In order to meet this challenge, much more systemic and perspicuous studies on the relationships between the photophysical properties and the optical limiting behaviors with different central metals and substituents need to be paid more attention. Our group have investigated the optical properties of α -substituted Al Pc and peripherally α - and β -substituted In Pcs [36,37], respectively, and conclude that the α -substituted Pcs have better optical limiting behaviors. In this present paper the photophysical and optical limiting properties of α -substituted Al, Ga and In Pcs have been studied systemically and elaborately, and the relationship between them has been analyzed, in order to obtain more effective guidelines for the practical applications of optical limiting materials.

2. Experimental

2.1. Materials and methods

All organic solvents were commercially available, dried and distilled by appropriate methods before use. ^1H NMR spectra were performed on a DPX400 Bruker FT-NMR spectrometer with DMSO- d_6 as solvent and tetramethylsilane (TMS) as internal standard. The mass spectra were obtained on a Biflex MALDI-TOF. Elemental analyses were performed on a Carlo Erba-1106 elemental analyzer. UV-vis absorption spectra were recorded on a Hitachi U-3010 spectrophotometer.

Fluorescence spectra were recorded on a Hitachi F-4500 fluorescence spectrophotometer. Fluorescence quantum yield (Φ_F) of S_1 state were determined by the comparative method using zinc Pc in 1-chloronaphthalene ($\Phi_F = 0.30$) as reference standard [38,39]. The fluorescence lifetimes of these Pcs were investigated with single-photon counting technique with an Edinburgh FL900 spectrophotometer.

Transient absorption at nanosecond time scale was investigated in argon-saturated THF solution at the concentration of 2×10^{-5} M. The excitation light was the harmonic of Nd:YAG laser (Continuum Surelite II, 355 nm and 7 ns FWHM). The signals were detected by Edinburgh LP900 and recorded on Tektronix TDS 3012B oscilloscope and computer. The triplet-minus-ground state extinction coefficient ($\Delta\epsilon_T$) were calculated by the method of total depletion or saturation [40,41]. The quantum yields of the triplet state were determined by the comparative method [42], using unsubstituted ZnPc in 1-chloronaphthalene as reference standard ($\Phi_T = 0.65$). The triplet lifetimes were obtained by kinetic analysis of the transient absorption.

The optical limiting properties were measured by the standard setup of our previously reported method [36,37]. All Pcs of **4–9** were dissolved in THF with the same linear transmittance T_{lin} , and placed in a 1.0 cm path length quartz cell and the solutions were bubbled with pure Argon for about 30 min to remove the dissolved O_2 . A 532 nm nanosecond Nd:YAG laser (Continuum Surelite II, 7 ns FWHM) was used as the laser source.

2.2. Synthetic procedures

2.2.1. 3-(4-tert-Butylphenoxy)phthalonitrile (**2**)

Compound **2** was synthesized by a similar method in the published papers [36,37]. A mixture of 3-nitrophthalonitrile (6.9 g, 40 mmol), 4-tert-butylphenol (6.0 g, 40 mmol) and anhydrous potassium carbonate (22.0 g, 160 mmol) was added to 30 mL dry DMF and stirred at room temperature for 3 days under nitrogen condition. Then the reaction mixture was poured into 100 mL cold water, the precipitated crude product was collected by filtration

and crystallized from toluene to give 7.2 g (yield: 71.8%) of **2**. EI-MS: 276.3 (M^+); ^1H NMR (CDCl_3): δ (ppm) = 7.62 (t, 1H), 7.48 (d, 2H), 7.39 (d, 2H), 7.32 (d, 1H), 7.28 (d, 1H), 1.32 (s, 9H).

2.2.2. 3-(iso-Butoxy)phthalonitrile (**3**)

Compound **3** was synthesized by a similar method in the published papers [36,37]. A mixture of 3-nitrophthalonitrile (6.9 g, 40 mmol), iso-butanol (5.9 mL, 48 mmol) and anhydrous potassium carbonate (22.0 g, 160 mmol) was added to 30 mL dry DMF and stirred at room temperature for 3 days under nitrogen condition, then the reaction mixture was poured into 100 mL cold water, the precipitated crude product was collected by suction filtration and crystallized with a little toluene to give 5.4 g (yield: 75.0%) of **3**. EI-MS: 200.1 (M^+); ^1H NMR (CDCl_3 , 400 Hz): δ (ppm) = 7.66 (t, 1H), 7.37 (d, 1H), 7.28 (d, 1H), 4.08 (d, 2H), 1.81–1.85 (m, 1H), 1.53 (d, 6H).

2.2.3. Tetra- α -(4-tert-butylphenoxy) aluminum phthalocyanine (**4**)

Compound **2** (2.8 g, 10 mmol) was added to 30 mL dry 1-pentanol with 1.5 mL 1,8-diazabicyclo[5.4.0]undec-7-ene (DBU) as a catalyst. The mixture was stirred at 60 °C for 1 h under a nitrogen atmosphere and then 0.4 g (3 mmol) of anhydrous AlCl_3 was added. The mixture was slowly brought to boiling over 1 h and then refluxed for 36 h, after the reactant was cooled to room temperature, 60 mL of methanol/water (1/1) mixture was added, the blue precipitated product was filtered, and washed with hydrochloric acid (5%, 50 mL), then 50 mL methanol, the crude product was purified by a silica-gel column chromatography with chloroform/ethanol (20:1) as eluent. Then the final product was dried at 50 °C under vacuum overnight to give 1.8 g (yield: 54.0%) of **4** ($\text{C}_{72}\text{H}_{64}\text{N}_8\text{O}_4\text{AlCl}$). UV-vis (THF) λ_{max} : 705, 334 nm; MALDI-TOF: 1167.1 (M^+), 1132.0 ($M^+ - \text{Cl}$); ^1H NMR (DMSO- d_6 , 400 Hz): δ (ppm) = 9.25–9.28 (m, 4H), 8.61–8.70 (m, 4H), 8.19–8.35 (m, 8H), 7.38–7.43 (m, 8H), 7.13–7.24 (m, 4H), 1.26–1.37 (d, 36H); Anal. Calcd. (%) for $\text{C}_{72}\text{H}_{64}\text{N}_8\text{O}_4\text{AlCl}$: C 74.06, H 5.48, N 9.60; found C 74.01, H 5.64, N 9.85.

2.2.4. Tetra- α -(4-tert-butylphenoxy) gallium phthalocyanine (**5**)

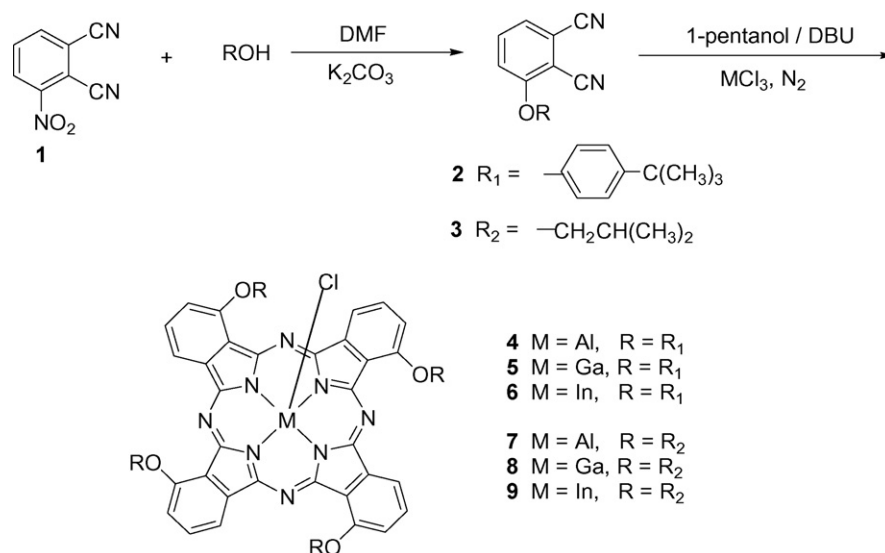
Compound **5** was prepared by a similar method to compound **4** in 71.8% yield ($\text{C}_{72}\text{H}_{64}\text{N}_8\text{O}_4\text{GaCl}$). UV-vis (THF) λ_{max} : 712, 336 nm; MALDI-TOF: 1209.6 (M^+), 1173.5 ($M^+ - \text{Cl}$); ^1H NMR (DMSO- d_6 , 400 Hz): δ (ppm) = 9.26–9.40 (m, 4H), 8.72–8.86 (m, 4H), 8.25–8.45 (m, 8H), 7.35–7.44 (m, 8H), 7.11–7.13 (m, 4H), 1.27–1.37 (d, 36H); Anal. Calcd. (%) for $\text{C}_{72}\text{H}_{64}\text{N}_8\text{O}_4\text{GaCl}$: C 71.43, H 5.29, N 9.26; found C 71.49, H 5.51, N 9.39.

2.2.5. Tetra- α -(4-tert-butylphenoxy) indium phthalocyanine (**6**)

Compound **6** was prepared by a similar method to compound **4** in 64.0% yield ($\text{C}_{72}\text{H}_{64}\text{N}_8\text{O}_4\text{InCl}$). UV-vis (THF) λ_{max} : 720, 351 nm; MALDI-TOF: 1254.7 (M^+), 1219.7 ($M^+ - \text{Cl}$); ^1H NMR (DMSO- d_6 , 400 Hz): δ (ppm) = 9.16–9.33 (m, 4H), 8.55–8.70 (m, 4H), 7.91–7.22 (m, 8H), 7.32–7.38 (m, 8H), 7.09–7.15 (m, 4H), 1.24–1.35 (d, 36H); Anal. Calcd. (%) for $\text{C}_{72}\text{H}_{64}\text{N}_8\text{O}_4\text{InCl}$: C 68.88, H 5.10, N 8.92; found C 68.96, H 5.45, N 8.53.

2.2.6. Tetra- α -(4-iso-butoxy) aluminum phthalocyanine (**7**)

Compound **3** (1.7 g, 5 mmol) was added to 30 mL dry 1-pentanol with 1.5 mL 1,8-diazabicyclo[5.4.0]undec-7-ene (DBU) as a catalyst. The mixture was stirred at 60 °C for 1 h under a nitrogen atmosphere and then 0.27 g (2 mmol) of anhydrous AlCl_3 was added. The mixture was slowly brought to boiling over 1 h and then refluxed for 36 h, after the reactant was cooled to room temperature, 30 mL of methanol/water (1:1) mixture was added, the precipitated blue product was filtered, and washed with hydrochloric acid (5%, 50 mL), then 50 mL methanol, the crude product was purified by a silica-gel column with chloroform/ethanol (20:1) as eluent. Then



Scheme 1. Synthetic routes of the Pcs 4–9.

the final product was dried at 50 °C under vacuum overnight to give 0.72 g (yield: 66.9%) of **7** (C₄₈H₄₈N₈O₄AlCl). UV–vis (THF) λ_{max}: 711, 323 nm; MALDI-TOF: 862.3 (M⁺), 826.1 (M⁺–Cl); ¹H NMR (DMSO-d₆, 400 Hz): δ (ppm) = 8.89–9.13 (d, 4H), 8.11–8.25 (t, 4H), 7.77–7.98 (d, 4H), 4.34–4.46 (d, 8H), 2.68–2.79 (m, 4H), 1.43–1.49 (d, 24H); Anal. Calcd. (%) for C₄₈H₄₈N₈O₄AlCl: C 66.78, H 5.56, N 12.98; found C 67.08, H 5.61, N 13.14.

2.2.7. Tetra-α-(4-iso-butoxyl) gallium phthalocyanine (**8**)

Compound **8** was prepared by a similar method to compound **7** in 78.0% yield (C₄₈H₄₈N₈O₄GaCl). UV–vis (THF) λ_{max}: 718, 325 nm; MALDI-TOF: 905.1 (M⁺), 869.5 (M⁺–Cl); ¹H NMR (DMSO-d₆, 400 Hz): δ (ppm) = 8.85–8.98 (d, 4H), 8.18–8.32 (t, 4H), 7.79–8.01 (d, 4H), 4.54–4.56 (d, 8H), 2.72–2.85 (m, 4H), 1.45–1.58 (d, 24H); Anal. Calcd. (%) for C₄₈H₄₈N₈O₄GaCl: C 63.61, H 5.36, N 12.37; found C 63.92, H 5.37, N 12.54.

2.2.8. Tetra-α-(4-iso-butoxyl) indium phthalocyanine (**9**)

Compound **9** was prepared by a similar method to compound **7** in 71.0% yield (C₄₈H₄₈N₈O₄InCl). UV–vis (THF) λ_{max}: 724, 325 nm; MALDI-TOF: 949.6 (M⁺), 914.6 (M⁺–Cl); ¹H NMR (DMSO-d₆, 400 Hz): δ (ppm) = 9.10–9.13 (d, 4H), 8.28–8.32 (t, 4H), 7.80–7.91 (d, 4H), 4.55–4.58 (d, 8H), 2.81–2.88 (m, 4H), 1.61–1.66 (d, 24H); Anal. Calcd. (%) for C₄₈H₄₈N₈O₄InCl: C 60.63, H 5.05, N 11.80; found C 60.71, H 4.63, N 11.93.

2.3. Preparation of glass matrix samples doped with Pcs

The glass matrixes were prepared by sol–gel technique with our improved methods. A mixture of tetraethyl orthosilicate (TEOS), 2,3-epoxypropoxy propyltrimethoxysilicane (KH560), and water (pH 2) in a weighing bottle was stirred at room temperature for 2 h, then a selected volume of MPcs in CH₂Cl₂ was added and stirred unsealed for another 4 h. Then it was transferred to a desiccator and degassed, then dried for 2 weeks to give a homogeneous and transparent MPC glass matrix.

3. Results and discussion

3.1. Synthesis

As shown in Scheme 1, three different central metal (Al, Ga and In) Pcs with two type of peripheral substituents (R₁ and R₂)

were synthesized. A mixture of 3-nitrothalonitrile **1** and 4-tert-butylphenol or iso-butanol in dry DMF was stirred at room temperature in the presence of K₂CO₃, to obtain the substituted dinitriles **2** or **3**. The cyclization of the dinitriles resulted in the corresponding Pcs in 1-pentanol solvent at 130 °C using DBU as catalyst under N₂ atmosphere. The obtained Pcs were purified by silica-gel column and then sublimated under vacuum. All obtained Pcs were characterized by elemental analysis and spectroscopic methods including UV–vis, ¹H NMR and MALDI-TOF, which are consistent with the proposed structures. Due to the two different (3- or 6-) substitutional positions, the Pcs obtained are actually a kind of mixtures of four constitutional isomers for each compound, and the ¹H NMR spectra of some compounds show multiplets signals. Its difficult to separate these isomers with column chromatography or high performance liquid chromatography (HPLC). However, the photophysical and optical limiting properties will not be different between these isomers [43]. Its worth to point out that these Pcs exhibit excellent solubility in most of organic solvents such as ethanol, methanol, THF, chloroform, DMF and DMSO, which is suitable for the investigation of photophysical and optical limiting properties in solution.

3.2. Ground state absorption and fluorescence emission

The UV–vis absorption spectra of **4–9** were measured in THF solutions at 4 × 10^{−6} M. As metal Pcs, the ground state absorptions of **4–9** have an intense S₀–S₁ transition with a small shoulder (Q

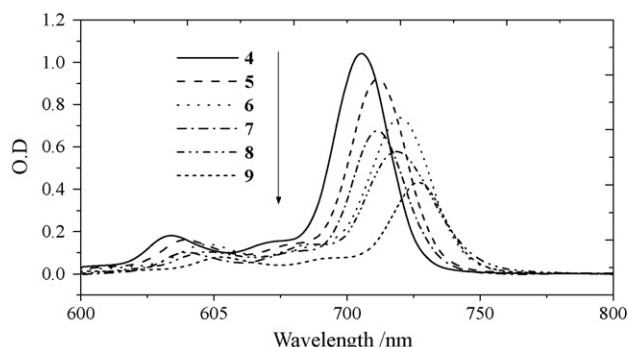
Fig. 1. Ground state absorption spectra of **4–9** in the range of 600–800 nm (Q bands).

Table 1
Photophysical parameters of **4–9**.

| | λ (Q) (nm) | λ (B) (nm) | ϵ (Q) ($M^{-1} cm^{-1}$) | ϵ (B) ($M^{-1} cm^{-1}$) | Emission (S_1) (nm) | Emission (S_2) (nm) | $\Phi_F(S_1)$ | $\tau_F(S_1)$ (ns) |
|----------|--------------------|--------------------|-------------------------------------|-------------------------------------|-------------------------|-------------------------|---------------|--------------------|
| 4 | 705 | 334 | 2.6×10^5 | 5.7×10^4 | 719 | 431 | 0.197 | 5.85 |
| 5 | 712 | 336 | 2.3×10^5 | 5.2×10^4 | 726 | 432 | 0.078 | 2.98 |
| 6 | 720 | 351 | 1.8×10^5 | 5.1×10^4 | 732 | 430 | 0.008 | 0.51 |
| 7 | 711 | 323 | 1.7×10^5 | 4.8×10^4 | 720 | 433 | 0.314 | 5.62 |
| 8 | 718 | 325 | 1.5×10^5 | 4.6×10^4 | 724 | 430 | 0.080 | 2.90 |
| 9 | 724 | 325 | 1.1×10^5 | 4.3×10^4 | 731 | 430 | 0.033 | 0.39 |

band) in the red region and a broad Soret band at 320–360 nm (B band). Fig. 1 shows that the Q band absorptions shift to longer wavelength with the central metals changing from Al to In. Furthermore, the Q bands of 4-iso-butoxy substituted Pcs **7–9** display much greater red shifts than that of 4-tert-butylphenoxy substituted Pcs **4–6**.

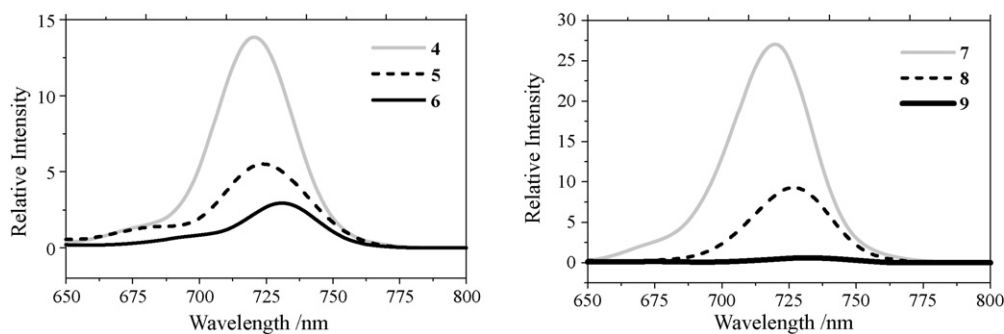
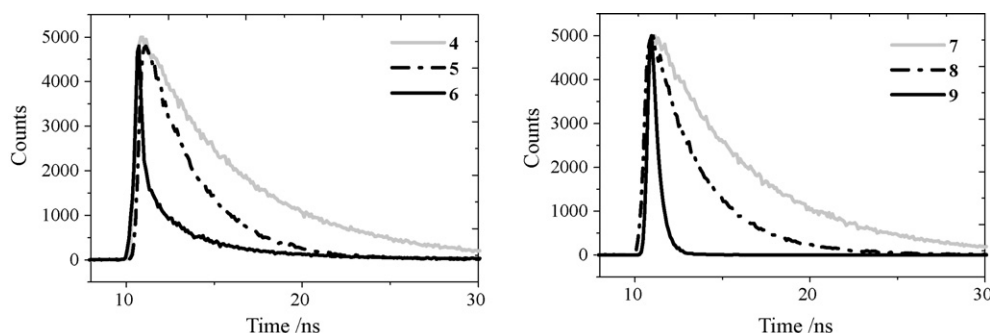
The Q band absorption can be directly ascribed to the transition from the HOMO to the LUMO [33], its red shift can be explained in terms of a decrease of the energy gap (ΔE) between HOMO and LUMO which lies on the π -electron density of the conjugation system [27,44]. In the metal Pcs the four equatorial donor atoms are provided by the monoanionic Pcs ligand, the central metal atom is an electron acceptor, the intensity of the formed coordination bonds, M–N, should dependent on the bound metal atoms. With increasing the atomic number of the metals in a same family, such as from Al to In, their electron negativity suffers little change, but the M–N bonds become more and more weaker, and therefore the higher π -electron density of the system and the lower energy gap (ΔE) between HOMO and LUMO are observed for the heavier central metal Pcs [27,44]. The fact indicates that the S_1 state energy get lower with the central metals changing from Al to In. In addition, the difference of the Q band between the two different peripheral substituted Pcs can be ascribed to their electron donor abilities. For the two different substituents, the 4-tert-butylphenoxy group displays weaker electron donor ability than that of 4-iso-butoxy group, which result in lower π -electron density of the conjugation

system and higher HOMO/LUMO energy positions of S_1 state for the 4-tert-butylphenoxy substituted Pcs (also shown in Fig. 6).

All the Pcs **4–9** exhibit good solubility in most solvents and their molar extinction coefficient (ϵ) of Q band (in THF) were estimated (Table 1). Pcs of **4–6** display better solubility than **7–9**, due to the larger volume of the 4-tert-butylphenoxy group which enhances the molecular mutual repency and makes the Pc rings difficult to be aggregated. For different central metals, the ϵ values of Q band follow the trend of Al > Ga > In. This fact suggests that Al-Pc have the lowest linear transmittance than Ga and In Pcs. In addition, for the two different substituted Pcs, **4–6** possess higher values of ϵ (Q band) than that of **7–9**.

The fluorescence emission spectra ($\lambda_{ex} = 610$ nm) were measured in THF solutions, which is summarized in Fig. 2 and Table 1 and indicate that changing the central metal from Al to In led to remarkable reduction of the fluorescence emission quantum yields. Moreover, the $\Phi_F(S_1)$ values of Pcs (**4–6**) are a bit smaller than that of (**7–9**). All Pcs **4–9** present short lifetimes of the S_1 state at nanosecond scale as shown in Fig. 3 and Table 1. Similar change is observed for the S_1 state lifetimes of different central metals, decreasing remarkably from Al to In.

The values of $\Phi_F(S_1)$ vary much upon the central metals, which is attributed to the heavy atom effect. Because of different spin-orbit coupling for different metals, the heavier the central metal is, the stronger the spin-orbit coupling and the shorter the energy gap between S_1 and T_1 states, and therefore the more probability

**Fig. 2.** The fluorescence emission spectra of **4–9** in argon-saturated THF solutions at 4×10^{-6} M with excited wavelength at 610 nm.**Fig. 3.** Decay profiles of S_1 fluorescence for **4–9**.

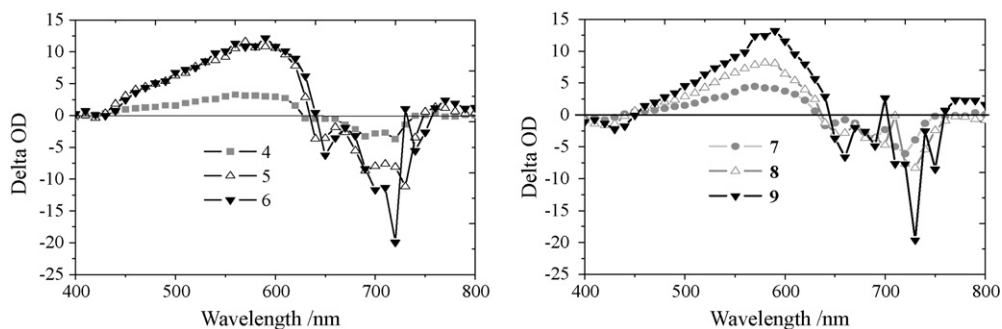


Fig. 4. Transient absorption spectra of 4–9, the spectra of 4–8 were recorded at 22.0 μs after excitation, and 9 was recorded at 24.0 μs after excitation.

Table 2
Photophysical parameters of triplet state.

| Compounds | $\lambda_{\text{max}} (T_n)$ (nm) | ϵ_0 ($\text{M}^{-1} \text{cm}^{-1}$) | $\Delta\epsilon_T$ ($\text{M}^{-1} \text{cm}^{-1}$) | τ_T (μs) | k_{ST} (s^{-1}) | Φ_T |
|-----------|-----------------------------------|---|---|----------------------------|------------------------------|----------|
| 4 | 560 | 7.4×10^2 | 4.8×10^4 | 251.9 | 6.4×10^8 | 0.74 |
| 5 | 570 | 9.8×10^2 | 1.7×10^5 | 87.3 | 3.9×10^9 | 0.76 |
| 6 | 590 | 5.9×10^2 | 1.8×10^5 | 21.8 | 2.3×10^{11} | 0.90 |
| 7 | 570 | 3.1×10^3 | 6.6×10^4 | 140.9 | 3.5×10^8 | 0.62 |
| 8 | 580 | 7.6×10^2 | 1.3×10^5 | 71.3 | 2.8×10^9 | 0.65 |
| 9 | 590 | 1.4×10^3 | 2.0×10^5 | 19.2 | 5.6×10^{10} | 0.73 |

of intersystem crossing from S_1 to T_1 states. Concerning the Pcs 4–6, the presence of 4-tert-butylphenoxy substituted bulky group enhances the internal vibration of Pc molecules, which increases the internal conversion (IC), and shows a bit lower values of $\Phi_T(S_1)$ than that of 4-iso-butoxy substituted Pcs 7–9.

3.3. Transient absorption

Transient absorption excited at 355 nm was investigated in argon-saturated THF solutions. As shown in Fig. 4, the broad positive signals are the absorption from the excited state and the negative signals are the results of bleaching due to the transition from the ground state. All the Pcs 4–9 show a broad transient absorption of T_1-T_n transition from 450 to 620 nm. The λ_{max} of transient absorption are 560, 570 and 590 nm for 4, 5 and 6, and 570, 580 and 590 nm for 7, 8 and 9, respectively. Moreover, the triplet-minus-ground state extinction coefficients ($\Delta\epsilon_T$) [37] and the molar extinction coefficients of ground state absorption (ϵ_0) at 532 nm were obtained and summarized in Table 2. The values of $\Delta\epsilon_T$ are much higher than ϵ_0 , which would result in reverse saturable absorption and produce optical limiting effect. With regard to different central metals, In-Pcs have the highest value of $\Delta\epsilon_T$ than that of Al and Ga-Pcs. This indicates that the In-Pc is the easiest to achieve the absorption from T_1 to T_n than Al and Ga-Pcs, which would effectively cause the difference of optical limiting performance.

The decay profiles of triplet state were investigated and shown in Fig. 5. The triplet lifetimes obtained by kinetic analysis of the transient absorption are summarized in Table 2. Similar dependence of triplet state lifetimes on the different central metals were observed for 4–9, shortening remarkably from Al to In. In addition, 4-tert-butylphenoxy substituted Pcs 4–6 have longer lifetimes than that of 4-iso-butoxy substituted Pcs 7–9.

The quantum yield of triplet state formation Φ_T is assumed to be equal to the quantum yield of intersystem crossing (ISC) from S_1 to T_1 states Φ_{ST} . The Φ_T and the rate of intersystem crossing k_{ST} were evaluated [37] and summarized in Table 2. The Φ_T values are 0.74, 0.76 and 0.90 for 4, 5 and 6, and 0.62, 0.65 and 0.73 for 7, 8 and 9, respectively. For different central metal Pcs, the values of Φ_T and k_{ST} follow the trend of $\text{In} > \text{Ga} > \text{Al}$, while for the two series of peripherally substituted Pcs, 4–6 possess higher values of Φ_T and k_{ST} than that of 7–9. The results can be explained by the four-level model as shown in Fig. 6. On the one hand, the energy gap between S_1 and T_1 states follows the trend of $\text{Al} > \text{Ga} > \text{In}$. On the other hand, the different central metals produce different spin–orbit couplings due to the heavy atom effect. The k_{isc} values of the π -electron states increase with the atomic number of the central metal, permitting more efficient population of the triplet states [5,29]. This is the reason why In-Pc has the highest values of Φ_T and k_{ST} than those of Al-Pc and Ga-Pc.

Comparison of the two series of peripherally substituted Pcs, the S_1 state levels of 4-tert-butylphenoxy substituted Pcs (4–6) are

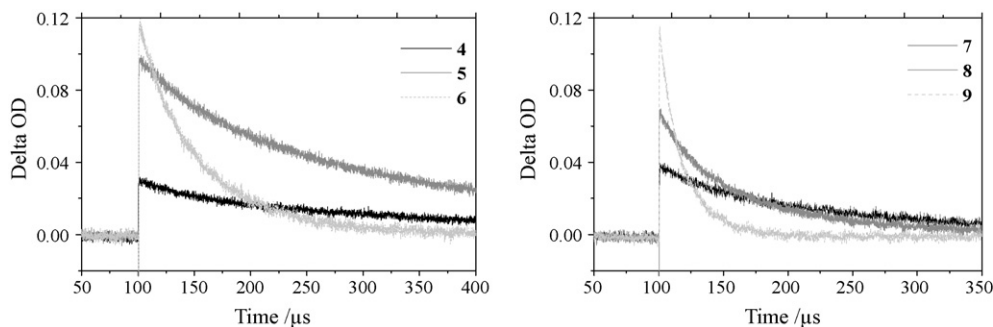


Fig. 5. Decay profiles of triplet state of 4–9.

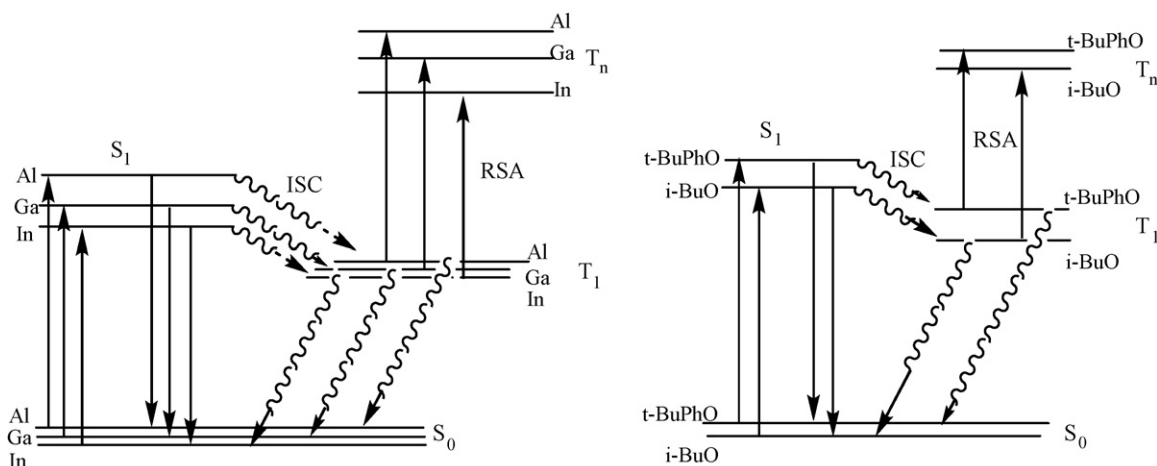


Fig. 6. The photophysical process model of the three different central metals (Al, Ga, In) Pcs (left) and two different substituted Pcs (4-tert-butylphenoxy and 4-iso-butoxy) (right).

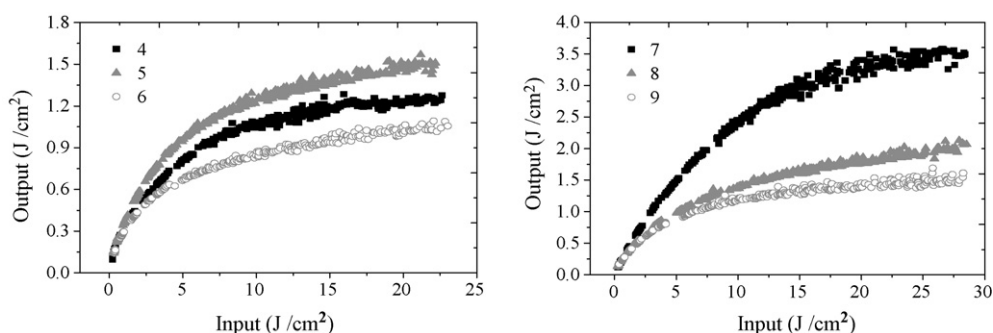


Fig. 7. Optical limiting responses for 7 ns pulses at 532 nm for 4–9.

a little higher than that of 4-iso-butoxy substituted Pcs (7–9) as shown in Fig. 6. However, compounds 4–6 display higher values of Φ_T and k_{ST} than that of 7–9, which can be explained in terms of changes in the conjugation of the Pc π system. The presence of phenyl group disturbs the π system of the Pc ring, which increases the intersystem crossing from S_1 to T_1 state [33].

The decay of molecules in T_1 state undergoes two pathways, one is intersystem crossing from T_1 to S_0 state in a nonradiative transition, another is going back to S_0 state via phosphorescence in a radiative transition. Because of the heavy atom effect, the consequence of increased intersystem crossing should shorten the triplet state lifetime [45]. This results in the remarkably decrease of τ_{T_1} in the order from Al to In. In addition, the 4-tert-butylphenoxy substituted Pcs have longer triplet lifetimes than that of 4-iso-butoxy substituted Pcs, which are due to the larger volume weakens the interactions of the Pc rings.

3.4. Optical limiting properties

Several parameters are introduced to evaluate the optical limiting characters. The linear transmittance T_{lin} which is the initial

transmittance of the sample, the limiting transmittance T_{lim} which is the lowest transmittance at the high input fluence, and the nonlinear attenuation factor (NAF) which is the ratio of the linear transmittance to the limiting transmittance T_{lin}/T_{lim} [36]. A high value of NAF gives a better optical limiting performance, and the nonlinear attenuation factors (NAF) can effectively reflect the optical limiting capability [46].

The optical limiting behaviors of 4–9 were investigated in argon-saturated THF solutions with the same linear transmittance (T_{lin}) of 74%. Fig. 7 shows that all the Pcs 4–9 exhibit outstanding optical limiting properties, the transmittance decrease remarkably with the increase of the input fluence. All the optical limiting parameters were estimated by the published method [36,37] as shown in Table 3. The Pcs 4–9 have the same linear transmittance but different limiting transmittance. The optical limiting capability of 4–9 followed the same sequence with NAF, i.e. 6 is a little better than 4 and 5, and 9 is better than 8 and 7. The optical limiting behaviors of two different substituted Pcs are shown in Fig. 8, which indicates that the 4-tert-butylphenoxy substituted Pcs 4–6 have higher values of NAF than those of 4-iso-butoxy substituted Pcs 7–9, which suggests better optical limiting behaviors for 4-tert-

Table 3
Parameters of optical limiting properties.

| Compounds | C/M | T_{lin} | T_{lim} | NAF | σ_0 (cm ²) | σ_{ex}^T (cm ²) | σ_{ex}^T/σ_0 |
|-----------|-----------------------|-----------|-----------|------|-------------------------------|------------------------------------|--------------------------|
| 4 | 1.72×10^{-4} | 74.6% | 4.9% | 15.2 | 2.82×10^{-18} | 2.11×10^{-17} | 7.5 |
| 5 | 1.28×10^{-4} | 74.8% | 5.6% | 13.3 | 3.71×10^{-18} | 2.58×10^{-17} | 7.0 |
| 6 | 2.29×10^{-4} | 74.3% | 4.3% | 17.2 | 2.24×10^{-18} | 1.69×10^{-17} | 7.6 |
| 7 | 4.29×10^{-4} | 73.8% | 11% | 6.65 | 1.17×10^{-18} | 4.09×10^{-18} | 3.5 |
| 8 | 1.73×10^{-4} | 73.9% | 7.2% | 10.2 | 2.94×10^{-18} | 2.15×10^{-17} | 7.3 |
| 9 | 9.70×10^{-5} | 73.6% | 5.1% | 14.0 | 5.37×10^{-18} | 3.94×10^{-17} | 7.4 |

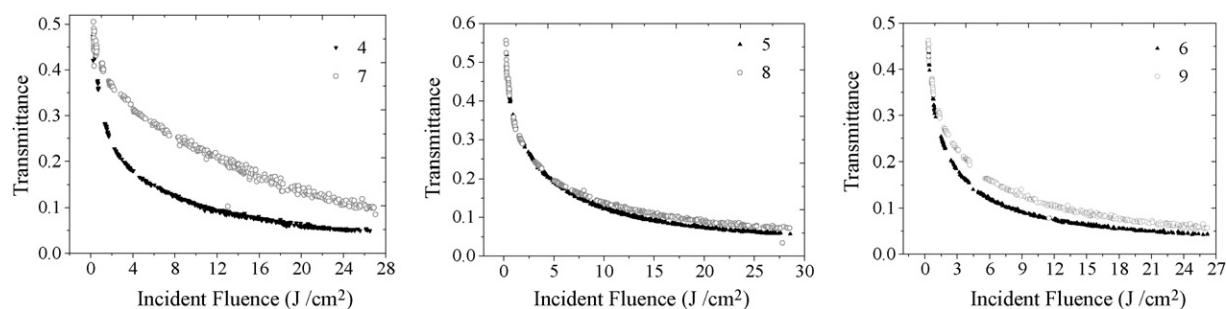


Fig. 8. Nonlinear transmittance responses of 4–6 (deep black) and 7–9 (light gray) to incident fluence at 532 nm, for 7 ns pulses.

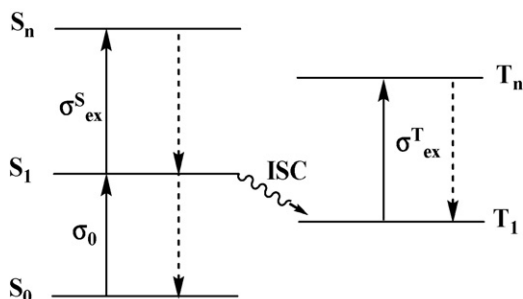


Fig. 9. Diagram description of the mechanism of reverse saturable absorption.

butylphenoxy substituted Pcs than that of 4-*iso*-butoxyl substituted Pcs.

The distinction of optical limiting behaviors of 4–9 is attributed to the difference of their photophysical properties such as Φ_T , $\Delta\epsilon_T$, ϵ_0 and τ_T , etc. In which the values of Φ_T and $\Delta\epsilon_T$ are key parameters. In Pcs 6 and 9 have the shortest lifetimes of triplet state τ_T and highest values of Φ_T and $\Delta\epsilon_T$, thus leading to the best optical limiting behaviors. Nevertheless, Al Pcs 4 and 7 have the longest τ_T but the lowest Φ_T and $\Delta\epsilon_T$, which cause not so good optical limiting behaviors in contrast to In Pcs. In addition, 4-*tert*-butylphenoxy substituted Pcs display better optical limiting behaviors than 4-*iso*-butoxyl substituted Pcs are the results of higher values of Φ_T , $\Delta\epsilon_T$ and τ_T . The longer lifetime of triplet state τ_T of the optical limiting material is necessary, but it is not determinant, the lifetime of triplet state τ_T on the scale of microseconds is good enough for the nanosecond optical limiting materials [36,37].

A five-level model (Fig. 9) is introduced to illustrate the mechanism of achieving optical limiting effect. The molecules at S_0 state absorb the first photon to S_1 state, then part of the S_1 state molecules undergo fast intersystem crossing to the T_1 state. When the irradiation is strong enough, the molecules continue to absorb another photon to reach the higher excited state S_n or T_n . When the excited

absorption cross section σ_{ex} is greater than that of the ground state σ_g , the progress is the so-called reverse saturable absorption, which is the origin of the optical limiting performance. However, for the nanosecond scale optical limiting, the S_1 to S_n absorption is weak enough to be ignored compared to the absorption of T_1 to T_n state [23]. Thus, the optical limiting behaviors of 4–9 greatly depend on the triplet state absorption from T_1 to T_n state. Accordingly, the ground state absorption cross section σ_0 and the triplet state absorption cross section σ_{ex}^T are also potent parameters to determine the optical limiting behaviors, a high ratio of σ_{ex}^T/σ_0 give a good optical limiting behavior [5,34]. The ratios σ_{ex}^T/σ_0 of 4–9 were estimated [36] as summarized in Table 3. Compounds 4, 5, 6, 8 and 9 have similar ratios of σ_{ex}^T/σ_0 , while the 7 has a smaller ratio of the σ_{ex}^T/σ_0 . All of the results are in consistent with the optical limiting behaviors of 4–9.

All the studies above were investigated in THF solutions. The results indicate that 4-*tert*-butylphenoxy substituted In-Pc exhibits the best optical limiting behavior. For the application of optical limiting behavior of Pcs, compounds 4–9 were solidified in glass matrix by sol-gel technique. The glass matrixes embed in the tailor-made quartz utensil are highly transparent, mechanically and thermodynamically stable, which is suitable for the investigation of photophysical and optical limiting properties. Most of important, the glass matrixes obtained by our improved methods are stable enough to stand against high laser fluence, about 30 J cm^{-2} in our experiment.

Fig. 10 shows the optical limiting behaviors of 5 and 6 in THF solutions and in glass matrixes. Both samples of 5 and 6 have the linear transmittance of 70% and 51%, respectively. The values of NAF for 5 and 6 are 22.6 and 25.9 in glass matrixes and 14.0 and 13.5 in THF solutions, respectively. In addition, the optical limiting thresholds for 5 and 6 are 0.31 and 0.21 (J cm^{-2}) in glass matrixes and 0.55 and 0.61 (J cm^{-2}) in THF solutions. It is obvious that the optical limiting performance is greatly improved in solid matrix, which renders the Pc-based materials for practical application.

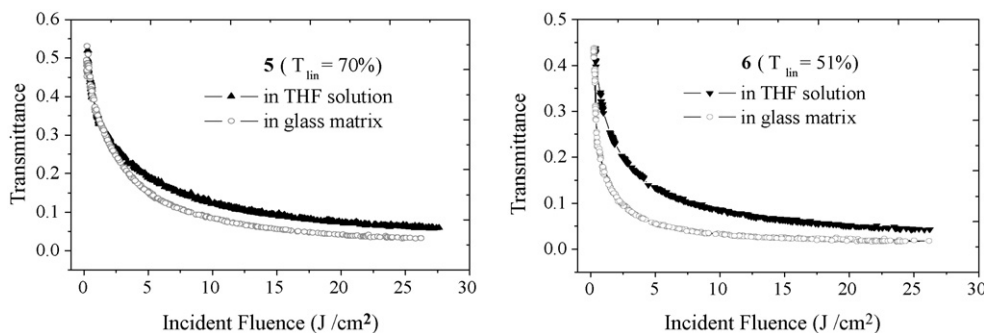


Fig. 10. Nonlinear transmittance responses of 5 and 6 in THF solutions and glass matrixes of 70% and 51% linear transmittance, respectively, to the incident fluence.

4. Conclusions

Six soluble of 4-tert-butylphenoxy and 4-iso-butoxyl substituted metal (Al, Ga and In) Pcs were synthesized, and their photophysical properties and optical limiting performance were evaluated and analyzed. Photophysical properties vary according to the different central metals and peripheral substituents, accordingly cause the difference of optical limiting behaviors. Taking the practical application of optical limiting into account, the promising optical limiting behaviors of Pcs are dependent on the ratio of $\sigma_{\text{ex}}^{\text{T}}/\sigma_0$, quantum yield of triplet state formation Φ_{T} and the triplet-minus-ground state extinction coefficient ($\Delta\epsilon_{\text{T}}$). Over all of these factors, the absorption of triplet state is one of the most important factors for a good optical limiting performance. By comprehensive investigation of the relationship between photophysical properties and optical limiting performance of the Pcs with different central metals and peripheral substituents, its concluded that the Pcs with heavier central metals may have better optical limiting performance owing to the enhanced spin-orbit coupling by heavy atom effect. The peripheral substituent with bulky group cannot only improve the solubility, but also weaken the intermolecular π - π interaction of Pc molecules and decrease the effect of internal conversion, which is significant to explore promising optical limiting materials. Moreover, solidified Pcs doped in the glass matrix which can greatly improve the optical limiting performance, and would be useful for the practical application of optical limiting materials.

Acknowledgements

This work was supported by the National Natural Science Foundation of China (Nos. 50773085, 20573122, 50221201) and the National Basic Research Program (2007CB808004). The authors thank the Laboratory of Organic Optoelectronic Functional Materials and Molecular Engineering, Technical Institute of Physics and Chemistry, CAS for their help.

References

- [1] M. Hanack, D. Dini, M. Barthel, S. Vagin, *Chem. Rec.* 2 (2002) 129–148.
- [2] S.J. Mathews, S. Chaitanya Kumar, L. Giribabu, S. Venugopal Rao, *Opt. Commun.* 280 (2007) 206–212.
- [3] D. Wöhrle, D. Meissner, *Adv. Mater.* 3 (1991) 129–138.
- [4] C.C. Leznoff, A.B.P. Lever (Eds.), *Phthalocyanines: Properties and Applications*, vols. 1–4, VCH Publishers, Inc., Cambridge, 1989, 1993, 1996.
- [5] G. de la Torre, P. Vázquez, F. Agulló-López, T. Torres, *Chem. Rev.* 104 (2004) 3723–3750.
- [6] J.W. Perry, K. Mansour, I.Y.S. Lee, X.L. Wu, P.V. Bedworth, C.T. Chen, D.K.P. Ng, S.R. Marder, P. Miles, T. Wada, M. Tian, H. Sasabe, *Science* 273 (1996) 1533–1536.
- [7] Y. Chen, N. He, J.J. Doyle, Y. Liu, X.D. Zhuang, W.J. Blau, *J. Photochem. Photobiol. A: Chem.* 189 (2007) 414–417.
- [8] L.W. Tutt, A. Kost, *Opt. Lett.* 18 (1993) 334–336.
- [9] M. Hanack, T. Schneider, M. Barthel, J.S. Shirk, S.R. Flom, R.G.S. Pong, *Coord. Chem. Rev.* 219–221 (2001) 235–258.
- [10] Y. Chen, M. Hanack, Y. Araki, O. Ito, *Chem. Soc. Rev.* 34 (2005) 517–529.
- [11] A. Slodek, D. Wöhrle, J.J. Doyle, W. Blau, *Macromol. Symp.* 235 (2006) 9–18.
- [12] M. Yükek, T. Ceyhan, F. Bağcı, H.G. Yağlıoğlu, A. Elmali, Ö. Bekaroğlu, *Opt. Commun.* 281 (2008) 3897–3901.
- [13] J.L. Brédas, C. Adant, P. Tackx, A. Persoons, B.M. Pierce, *Chem. Rev.* 94 (1994) 243–278.
- [14] L.W. Tutt, T.F. Boggess, *Prog. Quantum Electron* 17 (1993) 299–338.
- [15] Y. Chen, J. Doyle, Y. Liu, A. Strevens, Y. Lin, M.E. El-Khouly, Y. Araki, W.J. Blau, O. Ito, *J. Photochem. Photobiol. A: Chem.* 185 (2007) 263–270.
- [16] T. Xia, D.J. Hagan, A. Dogariu, A.A. Said, E.W. Van Stryland, *Appl. Opt.* 36 (1997) 4110–4122.
- [17] Y.P. Sun, J.E. Riggs, *Int. Rev. Phys. Chem.* 18 (1999) 43–90.
- [18] W. Blau, H. Byrnes, W.M. Dennis, J.M. Kelly, *Opt. Commun.* 56 (1985) 25–29.
- [19] D. Dini, M. Hanack, M. Meneghetti, *J. Phys. Chem. B* 109 (2005) 12691–12696.
- [20] L. De Boni, D.C.J. Rezende, C.R. Mendonça, *J. Photochem. Photobiol. A: Chem.* 190 (2007) 41–44.
- [21] D. Dini, M.J.F. Calvete, M. Hanack, R.G.S. Pong, S.R. Flom, J.S. Shirk, *J. Phys. Chem. B* 110 (2006) 12230–12239.
- [22] W. Sun, C.C. Byeon, M.M. McKerns, C.M. Lawson, G.M. Gray, D. Wang, *Appl. Phys. Lett.* 73 (1998) 1167–1169.
- [23] J.W. Perry, K. Mansour, S.R. Marder, K.J. Perry, D. Alvarez, I. Choong, *Opt. Lett.* 19 (1994) 625–627.
- [24] L. Bajema, M. Gouterman, B. Meyer, *J. Mol. Spectrosc.* 27 (1968) 225–235.
- [25] Y. Chen, M. Hanack, S.M. O’Flaherty, G. Bernd, A. Zeug, B. Roeder, W.J. Blau, *Macromolecules* 36 (2003) 3786–3788.
- [26] Z.Y. Li, X. Huang, S. Xu, Z.H. Chen, Z. Zhang, F.S. Zhang, K. Kasatani, *J. Photochem. Photobiol. A: Chem.* 188 (2007) 311–316.
- [27] N. Kobayashi, N. Sasaki, Y. Higashi, T. Osa, *Inorg. Chem.* 34 (1995) 1636–1637.
- [28] Y. Bian, R. Wang, J. Jiang, C.H. Lee, J. Wang, D.K.P. Ng, *Chem. Commun.* (2003) 1194–1195.
- [29] W. Sun, G. Wang, Y. Li, M.J.F. Calvete, D. Dini, M. Hanack, *J. Phys. Chem. A* 111 (2007) 3263–3270.
- [30] J.P. Linsky, T.R. Paul, R.S. Nohr, M.E. Kenney, *Inorg. Chem.* 19 (1980) 3131–3135.
- [31] H.L. Kee, J. Bhaumik, J.R. Diers, P. Mroz, M.R. Hamblin, D.F. Bocian, J.S. Lindsey, D. Holten, *J. Photochem. Photobiol. A: Chem.* 200 (2008) 346–355.
- [32] T. Nyokong, *Coord. Chem. Rev.* 251 (2007) 1707–1722.
- [33] Z. Musil, P. Zimcik, M. Miletin, K. Kopecky, P. Petrik, J. Lenco, *J. Photochem. Photobiol. A: Chem.* 186 (2007) 316–322.
- [34] M.J.F. Calvete, G.Y. Yang, M. Hanack, *Synth. Met.* 141 (2004) 231–243.
- [35] N. Kobayashi, *Coord. Chem. Rev.* 219–221 (2001) 99–123.
- [36] Q. Gan, S. Li, F. Morlet-Savary, S. Wang, S. Shen, H. Xu, G. Yang, *Opt. Express* 13 (2005) 5424–5433.
- [37] S. Wang, Q. Gan, Y. Zhang, S. Li, H. Xu, G. Yang, *Chem. Phys. Chem.* 7 (2006) 935–941.
- [38] A.T.R. Williams, S.A. Winfield, J.N. Miller, *Analyst* 108 (1983) 1067–1071.
- [39] W.R. Dawson, M.W. Windsor, *J. Phys. Chem.* 72 (1968) 3251–3255.
- [40] R. Bonneua, I. Carmichael, G.L. Hug, *Pure Appl. Chem.* 63 (1991) 289–299.
- [41] A.P. Pelliccioli, K. Henbest, G. Kwag, T.R. Carvagno, M.E. Kenney, M.A.J. Rodgers, *J. Phys. Chem. A* 105 (2001) 1757–1766.
- [42] R. Bensasson, C.R. Goldschmidt, E.J. Land, T.G. Trascott, *Photochem. Photobiol.* 28 (1978) 277–281.
- [43] N. Kobayashi, *Coord. Chem. Rev.* 219–221 (2001) 99–122.
- [44] H. Shinohara, O. Tsaryova, G. Schnurpfeil, D. Wöhrle, *J. Photochem. Photobiol. A: Chem.* 184 (2006) 50–57.
- [45] D. Atilla, N. Saydan, M. Durmus, A.G. Gürek, T. Khan, A. Rück, H. Walt, T. Nyokong, V. Ahsen, *J. Photochem. Photobiol. A: Chem.* 186 (2007) 298–307.
- [46] J.S. Shirk, R.G.S. Pong, S.R. Flom, H. Heckmann, M. Hanack, *J. Phys. Chem. A* 104 (2000) 1438–1449.